Frost, Ray L. and Palmer, Sara J. and Spratt, Henry J. (2009) *Synthesis and Raman spectroscopic study of Mg/Al,Fe hydrotalcites with variable cationic ratios.* Journal of Raman Spectroscopy, 40(9). pp. 1138-1143.

Synthesis and Raman spectroscopic study of Mg/Al,Fe hydrotalcites with variable cationic ratios

Sara J. Palmer, Ray L. Frost • and Henry J. Spratt

Inorganic Materials Research Program, School of Physical and Chemical Sciences, Queensland University of Technology, GPO Box 2434, Brisbane Queensland 4001, Australia.

Abstract

Hydrotalcites of formula $Mg_6(Fe,Al)_2(OH)_{16}(CO_3).4H_2O$ formed by intercalation with the carbonate anion as a function of divalent/trivalent cationic ratio have been successfully synthesised. The XRD patterns show variation in the d-spacing attributed to the size of the cation. Raman and infrared bands in the OH stretching region are assigned to (a) brucite layer OH stretching vibrations (b) water stretching bands and (c) water strongly hydrogen bonded to the carbonate anion. Multiple $(CO_3)^{2-}$ symmetric stretching bands suggest that different types of $(CO_3)^{2-}$ exist in the hydrotalcite interlayer. Increasing the cation ratio (Mg/Al,Fe) resulted in an increase in the combined intensity of the 2 Raman bands at around 3600 cm^{-1}, attributed to Mg-OH stretching modes, and a shift of the overall band profile to higher wavenumbers. These observations are believed to be a result of the increase in magnesium in the structure. Raman spectroscopy shows a reduction in the symmetry of the carbonate, leading to the conclusion that the anions are bonded to the brucite-like hydroxyl surface and to the water in the interlayer. Water bending modes are identified in the infrared spectra at positions greater than 1630 cm^{-1}, indicating the water is strongly hydrogen bonded to both the interlayer anions and the brucite-like surface.

KEYWORDS: hydrotalcite; pyroaurite; carbonate; Raman spectroscopy; vibrational spectroscopy; cation/anion substitution effects

INTRODUCTION

• Author to whom correspondence should be addressed (r.frost@qut.edu.au)

Hydrotalcites, or layered double hydroxides (LDHs) are fundamentally anionic clays, and are less well-known than cationic clays like smectites [1,2]. The structure of hydrotalcite can be derived from a brucite structure ($Mg(OH)_2$) in which e.g. Al^{3+} or Fe^{3+} (pyroaurite-sjögrenite) substitutes for the Mg^{2+}. This substitution creates a positive layer charge on the hydroxide layers, which is compensated by interlayer anions or anionic complexes [3,4]. When LDHs are synthesised any appropriate anion can be placed in the interlayer. These anions may be any anion with a suitable negative charge including the carbonate anion. The hydrotalcite may be considered as a gigantic cation, which is counterbalanced by anions in the interlayer. In hydrotalcites a broad range of compositions are possible of the type $[M^{2+}_{1-x}M^{3+}_x(OH)_2][A^{n-}]_{x/n}.yH_2O$, where M^{2+} and M^{3+} are the di- and trivalent cations in the octahedral positions within the hydroxide layers, with x normally between 0.17 and 0.33. It is normal practice to determine the composition of the formed hydrotalcite by chemical means such as ICP-AES or EDAX techniques. A^{n-} is an exchangeable interlayer anion [5]. In the natural hydrotalcites reevesite and pyroaurite, the divalent cations are Ni^{2+} and Mg^{2+} respectively with the trivalent cation being Fe^{3+}. In these cases, the carbonate anion is the major interlayer counter anion. Normally the hydrotalcite structure based upon takovite (Ni,Al) and hydrotalcite (Mg,Al) has basal spacings of ~8.0 Å where the interlayer anion is carbonate. Reevesite and pyroaurite are based upon the incorporation of carbonate into the interlayer with d(003) spacings of around 8 Å [6,7].

The reason for the potential application of hydrotalcites as catalysts rests with the ability to make mixed metal oxides at the atomic level, rather than at a particle level. Such mixed metal oxides are formed through the thermal decomposition of the hydrotalcite [8,9]. There are many other important uses of hydrotalcites such as in the removal of environmental hazards in acid mine drainage [10,11], and a mechanism for the disposal of radioactive wastes [12]. Their ability to exchange anions presents a system for heavy metal removal from contaminated waters [13]. The study of minerals, including hydrotalcites, by Raman spectroscopy has proven to be very useful [14-23]. Indeed, Raman spectroscopy has proven most useful for the study of diagenetically related minerals as often occurs with hydrotalcite minerals. Some previous studies have been undertaken by the authors using Raman spectroscopy to study hydrotalcites. Spectroscopic studies, especially Raman studies, of hydrotalcites are limited especially where large anions are involved. The aim of this paper is

to present Raman and infrared spectra of planned hydrotalcites with carbonate in the interlayer.

In this work, we report the synthesis of Mg/Al,Fe hydrotalcites with variable Mg/Al cation ratio. These synthetic materials are to be used to characterise hydrotalcites that form in Al^{3+} and Fe^{3+} rich solutions, such as in the Bayer industry. We also report the Raman and infrared spectroscopic analysis of hydrotalcite and explore the effect of divalent/trivalent ratio on hydrotalcite formation.

EXPERIMENTAL

Preparation of Mixed Metal Ion Solution

Varying amounts of aluminium chloride hexahydrate, iron(III) chloride hexahydrate and magnesium chloride hexahydrate are dissolved in 500 mL of water. The ratio of moles of M^{2+} to M^{3+}, where M is a metal cation, in the different solutions is 2:1, 3:1 and 4:1. The following Table summarises how much of each metal is dissolved in 500 mL of water. A caustic solution is also prepared, containing 2 M of sodium hydroxide and 0.2 M of sodium carbonate.

Insert Table 1 here

The chosen metal ion solution is then added at 40 mL/minute via a peristaltic pump. The combined solutions are then vacuum filtered, washed thoroughly with hot degassed water and dried in an oven overnight at 120 °C.

X-ray diffraction

X-Ray diffraction patterns of powdered samples are collected using a Philips X'pert wide angle X-Ray diffractometer, operating in step scan mode, with Co Kα radiation (1.78897Å).

Raman microscopy

The crystals of hydrotalcite are placed on the stage of an Olympus BHSM microscope, equipped with 10x and 50x objectives and are part of a Renishaw 1000 Raman microscope system, which also includes monochromators, a filter system and a charge coupled device (CCD). Raman spectra were excited by a HeNe laser (633 nm) at a nominal resolution of 2 cm^{-1} in the range between 100 and 4000 cm^{-1}. Repeated acquisition using the highest magnification is accumulated to improve the signal to noise ratio. Spectra are calibrated using the 520.5 cm^{-1} line of a silicon wafer. Previous studies by the authors provide more details of the experimental technique [24-29].

Infrared spectroscopy

Infrared spectra are obtained using a Nicolet Nexus 870 FTIR spectrometer with a smart endurance single bounce diamond ATR cell. Spectra over the 4000-525 cm^{-1} range are obtained by the co-addition of 128 scans with a resolution of 4 cm^{-1} and a mirror velocity of 0.6329 cm/s.

Spectral manipulation such as baseline adjustments, smoothing and normalisation are performed using the GRAMS® software package (Galactic Industries Corporation, Salem, NH, USA). Band component analysis is undertaken using the Jandel 'Peakfit' software package, which enables the type of fitting function to be selected and allows specific parameters to be fixed or varied accordingly. Band fitting is achieved using a Lorentz-Gauss cross-product function with the minimum number of component bands used for the fitting process. The Lorentz-Gauss ratio was maintained at values greater than 0.7 and fitting is undertaken until reproducible results were obtained with squared correlations of r^2 greater than 0.995.

RESULTS AND DISCUSSION

X-ray diffraction

The X-ray diffraction patterns for the carbonate interlayered hydrotalcites are shown in Fig. 1. EDX determined the hydrotalcite ratios to be 1.7, 2.7 and 4.0 for the 2:1, 3:1 and 4:1

hydrotalcites respectively. The XRD patterns prove that the hydrotalcites have been successfully synthesised. Hydrotalcite normally has a d(003) spacing of around 7.9 Å. The sulphate interlayered hydrotalcite has a spacing of 8.0 Å. There is an apparent small shift to higher d(003) spacings as the cation ratio increases. The greatest shift is observed when comparing the 2:1 HT with the 3:1 HT. The results obtained by EDX found that the Fe:Al concentration decreased as the overall Mg/Al,Fe ratio increased. It is not clearly understood as to why the change in cation ratio caused an increase in the d(001) spacing. Thus the XRD patterns show that the d-spacing for the carbonate interlayered hydrotalcite is cation dependent.

Vibrational spectroscopy

Only a very limited number of Raman studies have been reported so far on the interlayer carbonate anion in hydrotalcites. There are many examples of naturally occurring hydrotalcites with carbonate as the interlayer anion. When the carbonate species is present as a free ion, not involved in any bonding, it will exhibit a space group of D_{3h}. In the Raman spectrum one will observe $\nu_1(A'1)$, $\nu_3(E')$ and $\nu_4(E')$. As a result three bands, the bending non-planar mode $\nu_2(A''2)$, the anti-symmetrical stretching mode $\nu_3(E')$ and the bending angular mode $\nu_4(E')$, will be observed in the infrared spectrum around 880, 1415 and 680 cm^{-1}, while the symmetric stretching mode $\nu_1(A'1)$ is infrared inactive. However, changes can be expected when the carbonate ion is intercalated in the hydrotalcite structure as it will be affected by interactions with interlayer water molecules and/or OH-groups from the hydrotalcite layers. In comparison with free CO_3^{2-} a shift towards lower wavenumbers is generally observed. Interaction between interlayer water molecules and the carbonate ion is reflected by the appearance of bands at around 3000-3100 cm^{-1}, in the OH-stretching region of the infrared spectrum around 3000-3100 cm^{-1}

The Raman and infrared spectra may be conveniently divided into sections according to where the various vibrational bands are found. Thus the spectra are sectioned into (a) the OH stretching region, (b) the CO_3^{2-} stretching region and (c) the CO_3^{2-} bending region. The Raman and infrared spectra of the OH stretching region are displayed in Figs. 2 and 3 respectively. The spectra in these two figures may be contrasted. Water bands are not so easily observed in the Raman spectra of these hydrotalcites as water is a very poor Raman

scatterer. The intensity of the bands in Fig. 2 is therefore more likely to be associated with OH stretching bands. The intensity of the spectral profile in the infrared spectra is more likely to be associated with water stretching vibrations. The spectral profile is shifted to lower wavenumbers in the infrared spectrum. The Raman spectral profiles for the 2:1, 3:1 and 4: 1 are different. The peak maximum for the 2:1 hydrotalcite occurs at around 3513 cm^{-1}. The bands at 2908, 3094 and 3360 cm^{-1} are assigned to water stretching bands. The first band at 2908 cm^{-1} is attributed to water which is strongly hydrogen bonded to the carbonate anion. Such a unit is held within the hydrotalcite interlayer and serves to stabilise the hydrotalcite structure. The Raman bands for the 2:1 HT at 3513, 3592 and 3656 cm^{-1} are attributed to OH stretching vibrations of OH units bonded to the cations of the brucite-layer. The combined intensities of the two Raman bands at around 3600 cm^{-1}, increases as the divalent/trivalent cation ratio increases. It is proposed that the increase in intensity is due to a larger quantity of M-OH bonds within the structure, where M can be Mg, Al, Fe, or any permutation of these metals. A shift of the overall band profile to higher wavenumbers, as the cation ratio increases, is believed to be due to an increase in the quantity of Mg-OH bonds. Therefore, changes in the cationic ratio changes the Raman spectral profile in the OH stretching region.

In the infrared spectra of the OH stretching region (Fig.3) changes in the spectral profile are observed for the different hydrotalcites synthesised. The infrared bands for the 2:1 HT at 3074, 3275 and even 3439 cm^{-1} are assigned to water stretching bands. The higher wavenumber band at 3588 cm^{-1} may be attributed to the OH stretching bands of the Mg_3OH and Al_3OH units. The intensity of the bands at 3471 and 3596 cm^{-1} increase for the 3:1 HT. The intensity of the higher two wavenumber bands increases for the 4:1 HT. It is suggested that the two bands at 3043 and 3313 cm^{-1} for the 3:1 HT and at 3064 and 3337 cm^{-1} are due to water in two different environments in the HT interlayer. The lower wavenumber band is attributed to water which is reasonably strongly hydrogen bonded, possibly bonded to carbonate in the hydrotalcite interlayer.

An estimate of the intensity of the OH stretching vibrations may be obtained by an assessment of the type and number of MOH vibrations. In brucite type solids, there are tripod units M_3OH with several metals such as M, M', M". In hydrotalcites such as those based upon Mg and Zn of formula $Mg_xZn_{6-x}Al_2(OH)_{16}(CO_3).4H_2O$, a number of statistical permutations of the M_3OH units are involved. These are Mg_3OH, Zn_3OH, Al_3OH and

combinations such as Mg_2 ZnOH, Zn_2MgOH, Mg_2 AlOH, Al_2MgOH, Al_2 ZnOH, Zn_2AlOH, and even MgZnAlOH. These types of units will be distributed according to a probability distribution according to the composition. In this model, a number of assumptions are made, namely that the molecular assembly is random and that no islands or lakes of cations are formed. Such assembly is beyond the scope of this work but needs to be thoroughly investigated. In the simplest case namely $Mg_6Al_2(OH)_{16}(CO_3).4H_2O$ the types of units would be Mg_3OH, Mg_2AlOH, $MgAl_2OH$ and Al_3OH. A similar situation would exist for the $Mg_6Fe_2(OH)_{16}(CO_3).4H_2O$ hydrotalcite. In a somewhat oversimplified model, for the $Mg_6Fe_2(OH)_{16}(CO_3).4H_2O$ hydrotalcite, the most intense bands would be due to the Mg_3OH and Fe_3OH bands.

The Raman spectra of the synthesised hydrotalcites with different cationic ratios in the 950 to 1650 cm^{-1} region are shown in Fig. 4. The band at around 1059 cm^{-1} is assigned to the $(CO_3)^{2-}$ symmetric stretching mode. The band is not a simple band and may be subdivided into component bands as shown. The additional components are more readily observed in the Raman spectrum of the 4:1 HT. For the 2:1 HT three bands are observed at 1032, 1060 and 1091 cm^{-1}. The 1032 cm^{-1} band is assigned to a 'free' carbonate anion i.e. a carbonate anion which is not bonded to the brucite hydroxyl surface and water; the band at 1060 cm^{-1} is associated with carbonate anions bonded to the brucite hydroxyl surface; the higher wavenumber band at 1091 cm^{-1} is attributed to carbonate anions strongly hydrogen bonded to water. The three carbonate bands are found at 1022, 1058 and 1083 cm^{-1} for the 3:1 HT. The bands are observed at 1022, 1059 and 1076 cm^{-1} for the 4:1 HT. Bands assigned to carbonate strongly hydrogen bonded to water shift to lower wavenumbers as the cation ratio increases. This shift suggests that the bonding between carbonate and water is becoming stronger as the hydrogen bond distances decrease. Low intensity bands are observed in the 1200 to 1600 cm^{-1} region. For the 2:1 HT two bands are observed at 1212 and 1386 cm^{-1}; for the 3:1 HT two bands are observed at 1226 and 1384 cm^{-1} and for the 4:1 HT two Raman bands are found at 1254 and 1375 cm^{-1}. One probable assignment of these bands is to the $(CO_3)^{2-}$ antisymmetric stretching modes. The band at around 1588 cm^{-1} is considered to be due to water bending modes. Because the intensity of these bands is quite low, it is difficult to define exactly the position of these bands.

The infrared spectra of the three synthesised HTs are shown in Fig. 5. These spectra compliment the Raman spectra reported in Fig. 4. Interestingly no $(CO_3)^{2-}$ symmetric

stretching modes are observed. The very low intensity bands in the 1200 to 1600 cm^{-1} Raman spectral region show significantly greater intensity in the infrared spectrum. For the 2:1 HT two bands are observed at 1362 and 1413 cm^{-1}. For the 3:1 HT the bands are found at 1364 and 1474 cm^{-1} and for the 4:1 HT the bands are observed at 1367 and 1446 cm^{-1}. These bands are assigned to the $(CO_3)^{2-}$ antisymmetric stretching modes. The water bending mode at around 1640 cm^{-1} is more easily observed in the infrared spectrum as water has a very low scattering cross section in the Raman spectrum.

A comparison may be made with the band positions in other HTs and natural carbonates. The shift towards lower wavenumbers indicates a loss of freedom compared to free CO_3^{2-} and as a consequence a lowering of the carbonate symmetry occurs, from D_{3h} to probably C_{2s} or C_v. The Raman spectrum of takovite displays intense Raman band at 1060 cm^{-1} with a low intensity band at 1042 cm^{-1}. The position of this band may be compared with the values for witherite and cerrusite where positions of 1063 and 1053 cm^{-1} are observed. The infrared spectrum of takovite shows two bands at 1351 and 1417 cm^{-1}. As a result of this symmetry lowering the infrared inactive ν_1 mode will be activated. Indeed, a weak band has been observed around 1050-1060 cm^{-1}. In addition the ν_3 mode shows a small splitting in the order of 30-60 cm^{-1}. Some papers have only reported the activated ν_1 in combination with a single ν_3 band. In these cases the ν_3 band seems to be broadened due to an overlap of the two split modes ν_3 and ν_{3a}.

The Raman spectra in the 100 to 850 cm^{-1} region are shown in Fig. 6. The two bands at around 471 and 548 cm^{-1} are common to all three spectra. The bands are considered to be due to the linkage bonds, such as AlOAl and AlOMg linkage in the hydrotalcite. The bands observed in the Raman spectra at around 691 cm^{-1} is assigned to the $(CO_3)^{2-}$ ν_4 mode. Since the band is of low intensity, it is not possible to determine whether there is more than one band present in this spectral region. These low intensity bands are observed more clearly in the infrared spectrum (Fig. 5). For the 2:1 HT three infrared bands are noted at 604, 733 and 854 cm^{-1}; for the 3:1 HT infrared bands are observed at 590 and 691 cm^{-1} and for the 4:1 HT the bands are found at 576 and 673 cm^{-1}. These bands are assigned to the $(CO_3)^{2-}$ ν_4 mode. For takovite a band is observed at 687 cm^{-1} and is attributed to the ν_4 mode. However, for the ν_4 mode Kloprogge and Frost reported a minor sharp band at 694 cm^{-1}, which indicates a similar sized shift but in opposite direction. A reasonable explanation for this band is given

by Kagunya *et al.*, who showed the presence of a band at 698 and 695 cm^{-1} in the Raman spectra of Mg/Al-hydrotalcites with OH^- and CO_3^{2-} as interlayer anion, respectively and assigned this vibration as the $E_{g(T)}$ mode. [30] This band will then fully overlap the much weaker carbonate ν_4 mode. Detailed examination of the 694 cm^{-1} band indicates a rather sudden broadening supporting an overlap between these two bands. Similarly, Kagunya *et al.* gave an alternative assignment for the 1060 cm^{-1} band as the $E_{g(R)}$ (OH) mode, which they observed in both the carbonate and the hydroxyl interlayered LDHs. [30]

CONCLUSIONS

In this research we have shown that hydrotalcites with different cationic ratios (Mg/Al,Fe) can be successfully synthesised. By comparison of the X-ray diffraction patterns of the synthesised hydrotalcites with a standard reference pattern, it is proven that the hydrotalcites were synthesised. It is observed in XRD that increasing the cation ratio causes a change in the $d_{(003)}$ spacing due to the incorporation of the larger Fe^{3+} ions. The reason for this change is not known. Hydrotalcites have a unique structure in that the mineral acts like anionic clay with a 'giant' cation whose charge is counterbalanced by multiple anions in the interlayer. Hydrotalcites are normally not easy to measure in terms of Raman spectroscopy because of their small particle size together with their disordered nature.

In this work, both the Raman and infrared spectra of the interlayer anion of carbonate have been collected and the spectra related to the structure of the synthesised mineral. The hydroxyl stretching region of both Raman and infrared observed a shift and intensity changes, due to the increased number of Mg-OH bonds in the hydrotalcite structure. The splitting of the ν_3, ν_4 and ν_2 modes indicates symmetry lowering of the carbonate anions. The symmetry lowering must be taken into account through the bonding of the carbonate anions to both water and the brucite-like hydroxyl surface. Water plays an essential role in the hydrotalcite structure as may be evidenced by the position of the water bending modes. The water is strongly hydrogen bonded to both the anions and the hydroxyl surface. Raman spectroscopy has the advantage of water being a very poor scatterer and hence is difficult to observe compared with IR spectroscopy. Thus the cation OH stretching vibrations are more readily observed with Raman spectroscopy.

Acknowledgments

The financial and infra-structure support of the Queensland University of Technology, Inorganic Materials Research Program is gratefully acknowledged. . One of the authors (SJP) is grateful to RioTintoAlcan International Limited for a Masters scholarship. The Australian Research Council (ARC) is thanked for funding the instrumentation.

REFERENCES

1. Hashi K, Kikkawa S, Koizumi M *Clays and Clay Minerals* **1983**, *31*, 152-4.
2. Ingram L, Taylor HFW *Min. Mag.* **1967**, *36*, 465-79.
3. Taylor RM *Clay Minerals* **1982**, *17*, 369-72.
4. Taylor HFW *Min. Mag.* **1969**, *37*, 338-42.
5. Hansen HCB, Koch CB *App. Clay Sc.***1995**, *10*, 5-19.
6. Bish DL, Livingstone A *Min. Mag.* **1981**, *44*, 339-43.
7. Nickel EH, Clarke RM *Am. Min.* **1976**, *61*, 366-72.
8. Rey F, Fornes V, Rojo JM *J. Chem. Soc., Faraday Trans.* **1992**, *88*, 2233-8.
9. Valcheva-Traykova M, Davidova N, Weiss A *J. Mater. Sci.* **1993**, *28*, 2157-62.
10. Lichti G, Mulcahy J *Chem. Aust.* **1998**, *65*, 10-13.
11. Seida Y, Nakano Y *J. Chem. Eng. Japan* **2001**, *34*, 906-911.
12. Roh Y, Lee SY, Elless MP, Foss JE *Clay.Clay Min.* **2000**, *48*, 266-271.
13. Seida Y, Nakano Y, Nakamura Y *Water Res.* **2001**, *35*, 2341-2346.
14. Frost RL, Cejka J, Ayoko G *J. Raman Spectrosc.* **2008**, *39*, 495-502.
15. Frost RL, Cejka J, Ayoko GA, Dickfos MJ *J. Raman Spectrosc.* **2008**, *39*, 374-379.
16. Frost RL, Cejka J, Dickfos MJ *J. Raman Spectrosc.* **2008**, *39*, 779-785.
17. Frost RL, Cejka J, Keeffe EC, Dickfos MJ *J. Raman Spectrosc.* **2008**, *39*, 1413-1418.
18. Frost RL, Dickfos MJ, Cejka J *J. Raman Spectrosc.* **2008**, *39*, 582-586.
19. Frost RL, Dickfos MJ, Cejka J *J. Raman Spectrosc.* **2008**, *39*, 1158-1161.
20. Frost RL, Dickfos MJ, Reddy BJ *J. Raman Spectrosc.* **2008**, *39*, 1250-1256.
21. Frost RL, Hales MC, Wain DL *J. Raman Spectrosc.* **2008**, *39*, 108-114.
22. Frost RL, Keeffe EC *J. Raman Spectrosc.* **2008**, *in press*.
23. Frost RL, Keeffe EC *J. Raman Spectrosc.* **2008**, *39*, 1408-1412.
24. Frost RL, Locke A, Martens WN *J. Raman Spectrosc.* **2008**, *39*, 901-908.
25. Frost RL, Reddy BJ, Dickfos MJ *J. Raman Spectrosc.* **2008**, *39*, 909-913.
26. Hales MC, Frost RL, Martens WN *J. Raman Spectrosc.* **2008**, *39*, 1141-1149.
27. Palmer SJ, Frost RL, Ayoko G, Nguyen T *J. Raman Spectrosc.* **2008**, *39*, 395-401.
28. Zhao Y, Frost RL *J. Raman Spectrosc.* **2008**, *39*, 1494-1501.
29. Zhao Y, Yang J, Frost RL *J. Raman Spectrosc.* **2008**, *39*, 1327-1331.
30. Kagunya W, Baddour-Hadjean R, Kooli F, Jones W *Chem. Phys.***1998**, *236*, 225-234.

345

	2:1 Solution	*3:1 Solution*	*4:1 Solution*
Magnesium	67.765g	76.24g	81.32g
Aluminium	11.11g	8.335g	6.665g
Iron(III)	22.525g	16.895g	13.515g

346

347 **Table 1**

List of Fig.s

Fig. 1 X-ray diffraction patterns of the synthesised hydrotalcites with variable cationic ratios

Fig. 2 Raman spectra of the synthesised hydrotalcites with variable cationic ratios in the 2750 to 3750 cm^{-1} region

Fig. 3 Infrared spectra of the synthesised hydrotalcites with variable cationic ratios in the 2000 to 4000 cm^{-1} region

Fig. 4 Raman spectra of the synthesised hydrotalcites with variable cationic ratios in the 950 to 1650 cm^{-1} region

Fig. 5 Infrared spectra of the synthesised hydrotalcites with variable cationic ratios in the 500 to 1750 cm^{-1} region

Fig. 6 Raman spectra of the synthesised hydrotalcites with variable cationic ratios in the 100 to 600 cm^{-1} region

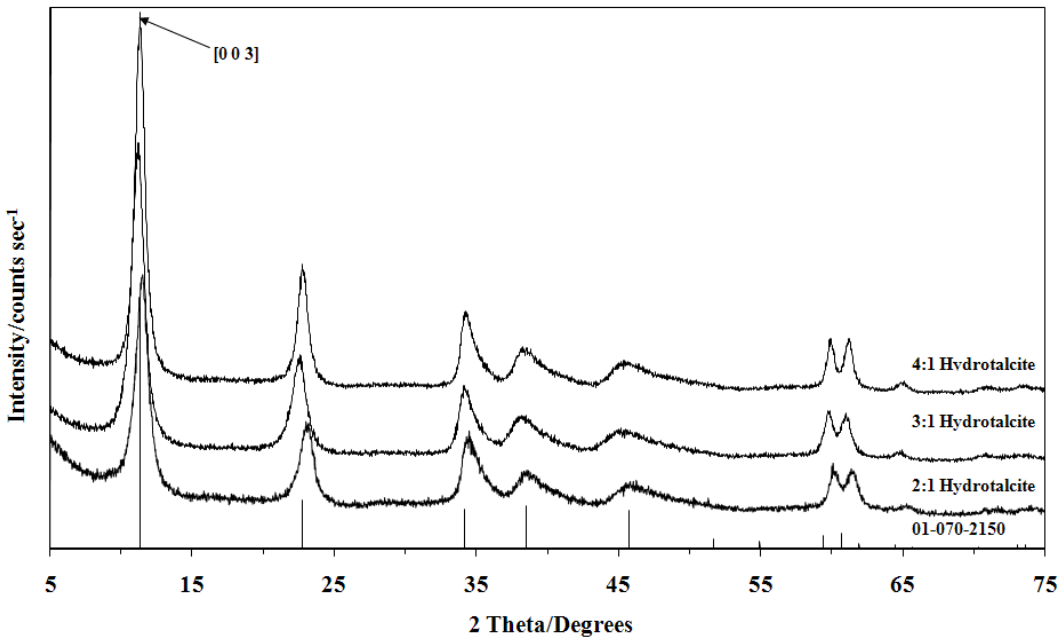

367

368

369

370 **Fig. 1**

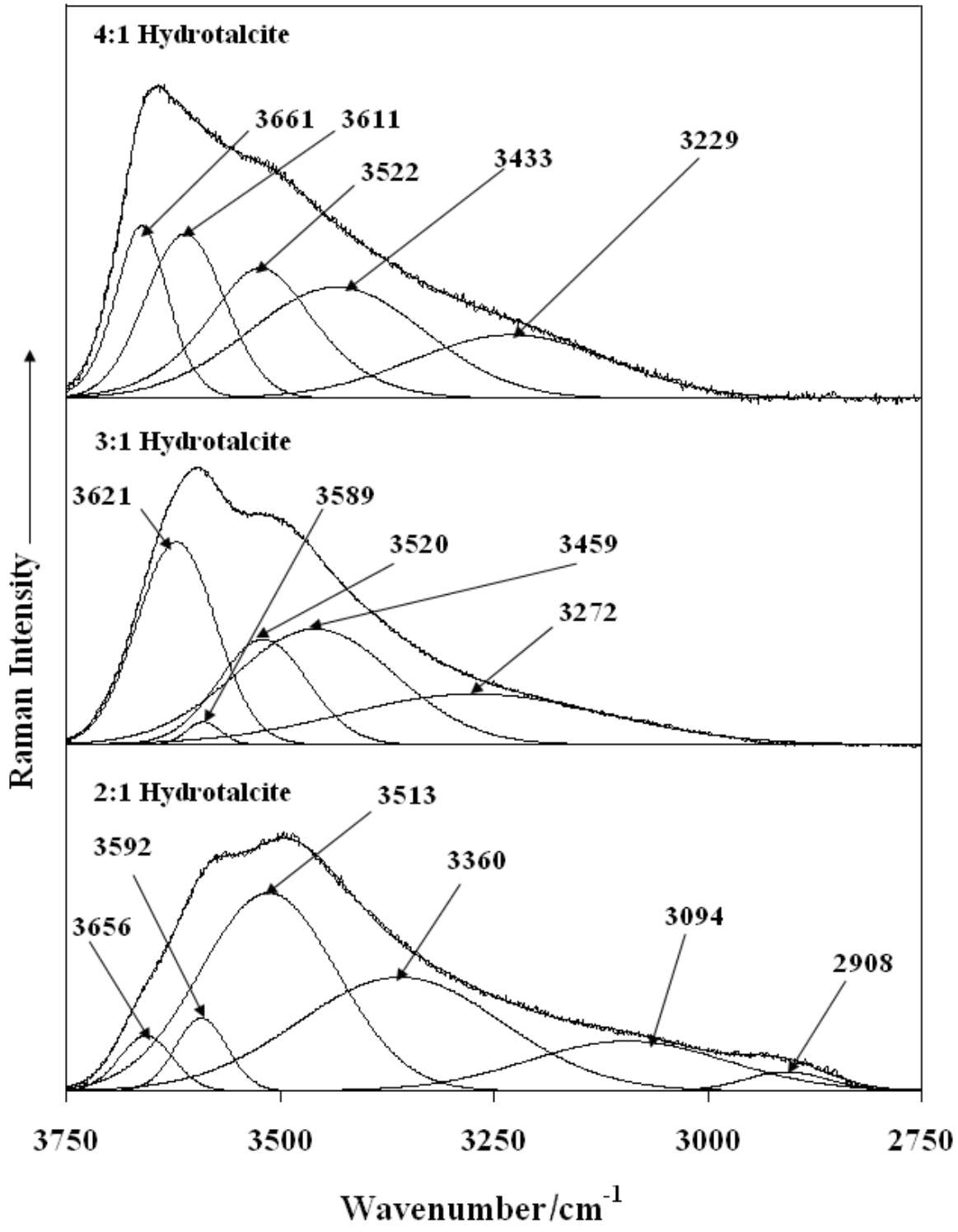

371

372 **Fig. 2**

373

374

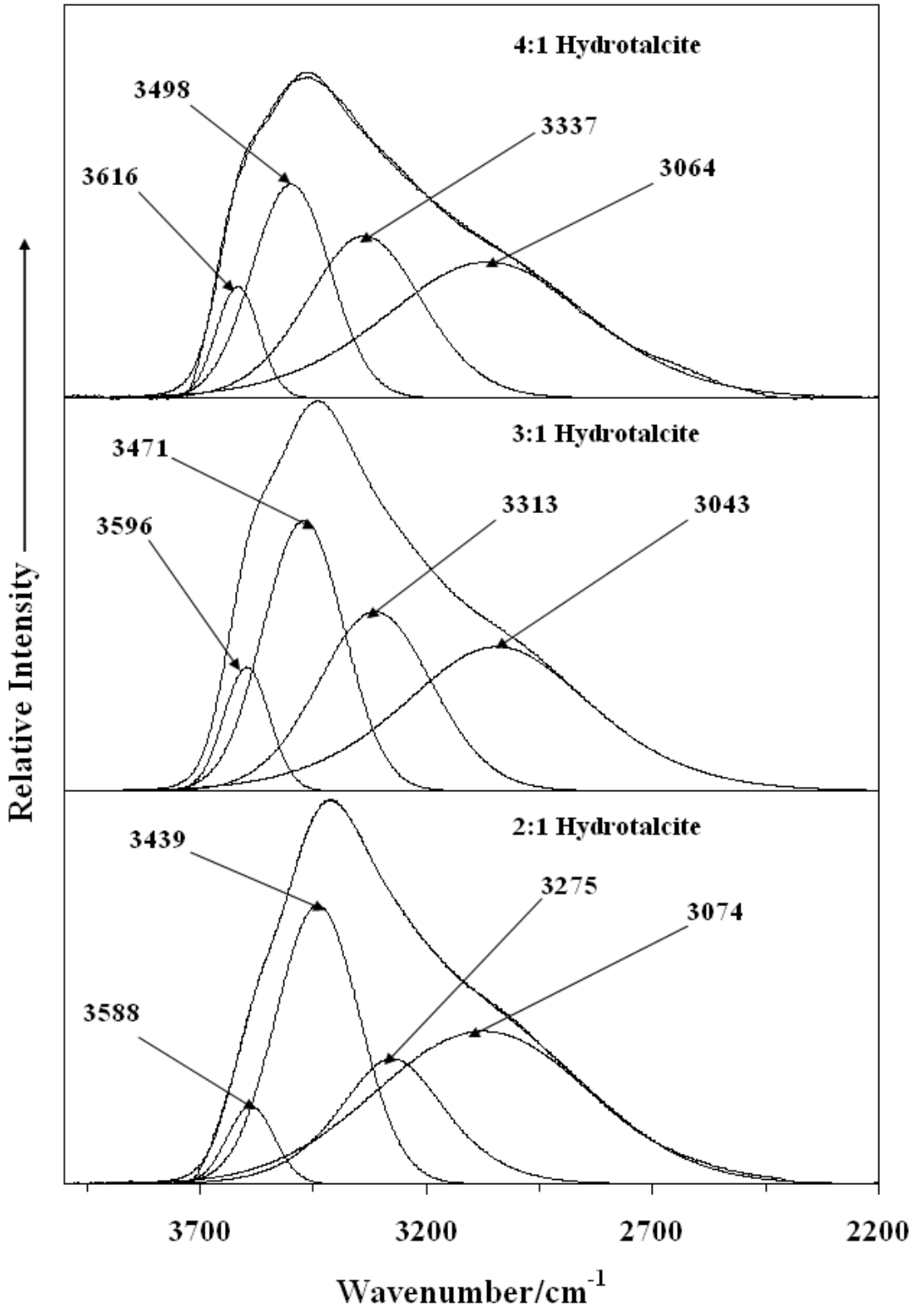

375

376

377 **Fig. 3**

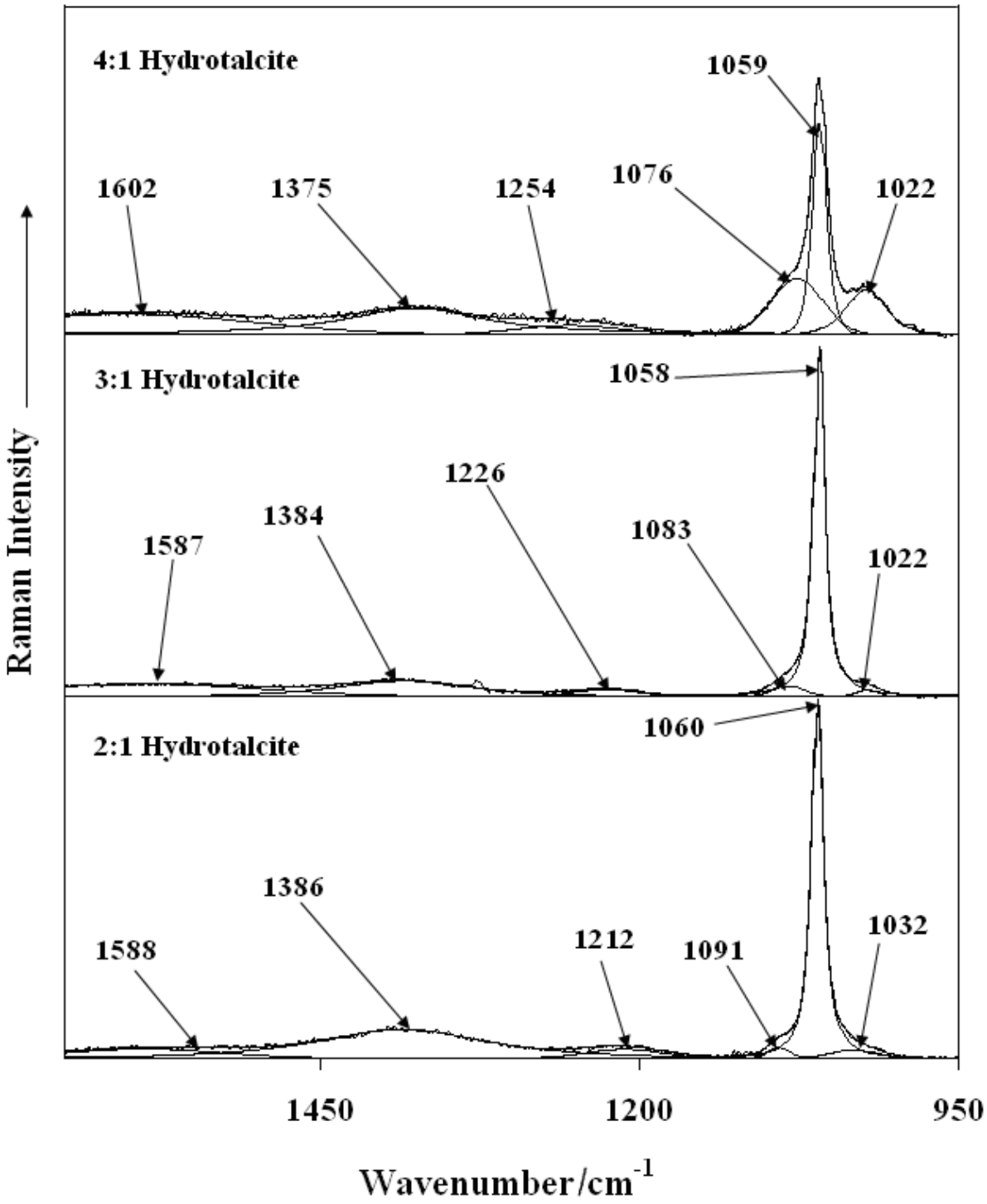
4:1 Hydrotalcite
1059
1602
1375
1254
1076
1022
3:1 Hydrotalcite
1058
1226
1384
1587
1083
1022
2:1 Hydrotalcite
1060
1386
1588
1212
1091
1032
Raman Intensity
1450
1200
950
Wavenumber/cm-1

Fig. 4

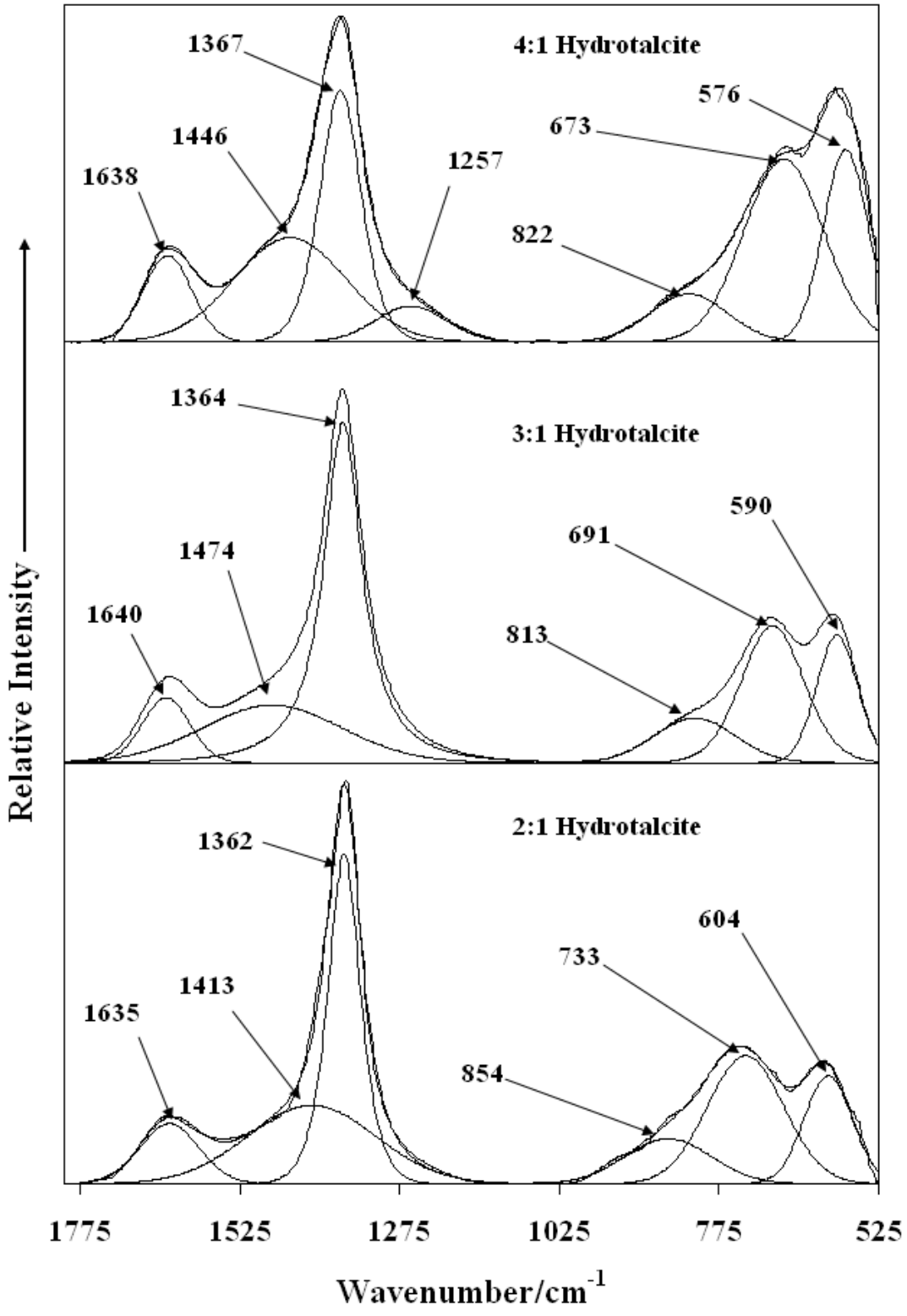
4:1 Hydrotalcite
1367
1446
1638
1257
576
673
822
3:1 Hydrotalcite
1364
1474
1640
590
691
813
2:1 Hydrotalcite
1362
1413
1635
604
733
854
Relative Intensity
1775
1525
1275
1025
775
525
Wavenumber/cm-1

Fig. 5

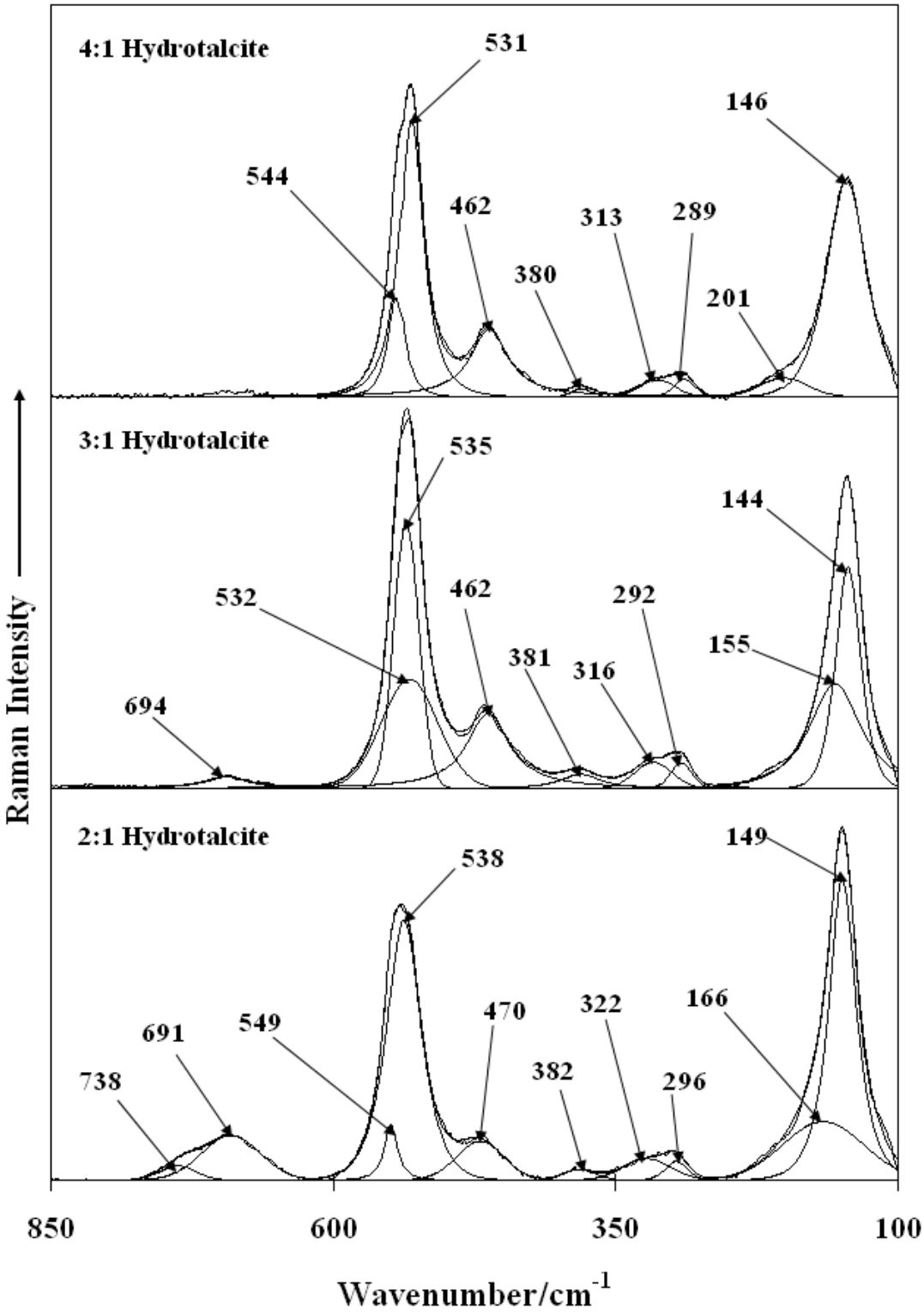
4:1 Hydrotalcite
531
146
544
462
313
289
380
201
3:1 Hydrotalcite
535
144
532
462
292
155
381
316
694
2:1 Hydrotalcite
538
149
691
549
470
322
166
738
382
296
Raman Intensity
850
600
350
100
Wavenumber/cm-1

Fig. 6